


RESEARCH

Open Access



Repair abilities of mouse autologous adipose-derived stem cells and ShakeGel™3D complex local injection with intrauterine adhesion by BMP7-Smad5 signaling pathway activation

Yun-xia Zhao¹ , Shao-rong Chen¹, Qiao-yi Huang¹, Wei-can Chen², Tian Xia³, Yan-chuan Shi^{4,5}, Hong-zhi Gao⁶, Qi-yang Shi^{1*} and Shu Lin^{4,7*}

Abstract

Background: The objective was to explore the therapeutic effect of autologous adipose-derived stem cells (ADSCs) combined with ShakeGel™3D transplantation to activate the BMP7-Smad5 signaling pathway to treat intrauterine adhesions (IUA).

Methods: Autologous ADSCs were isolated and then merged with ShakeGel™3D. The IUA model was established by mechanical injury. The third generation of autologous ADSCs was injected directly into the uterus in combination with ShakeGel™3D. After 7 days of treatment, endometrial morphology, number of endometrial glands, endometrial fibrosis area, and fibrosis biomarker analysis by RT-PCR and IHC were examined. BMP7 and phosphorylation of Smad5 were also detected, and the recovery of infertility function in treated mice was evaluated.

Results: Fluorescence-activated cell sorting (FACS) showed that autologous ADSCs expressed CD105 (99.1%), CD29 (99.6%), and CD73 (98.9%). Autologous ADSCs could still maintain a good growth state in ShakeGel™3D. Histological examination revealed that the number of endometrial glands increased significantly, and the area of fibrosis decreased. At the same time, the expression of BMP7 and Smad5 in the ADSCs + Gel group was significantly upregulated, and the final reproductive function of this group was partly recovered.

(Continued on next page)

* Correspondence: wsqy214@163.com; shulin1956@126.com

¹Department of Gynaecology and Obstetrics, The Second Affiliated Hospital of Fujian Medical University, No.34 North Zhongshan Road, Quanzhou 362000, Fujian Province, China

⁴Diabetes and Metabolism Division, Garvan Institute of Medical Research, 384 Victoria Street, Darlinghurst, Sydney, NSW 2010, Australia

Full list of author information is available at the end of the article



© The Author(s). 2021 **Open Access** This article is licensed under a Creative Commons Attribution 4.0 International License, which permits use, sharing, adaptation, distribution and reproduction in any medium or format, as long as you give appropriate credit to the original author(s) and the source, provide a link to the Creative Commons licence, and indicate if changes were made. The images or other third party material in this article are included in the article's Creative Commons licence, unless indicated otherwise in a credit line to the material. If material is not included in the article's Creative Commons licence and your intended use is not permitted by statutory regulation or exceeds the permitted use, you will need to obtain permission directly from the copyright holder. To view a copy of this licence, visit <http://creativecommons.org/licenses/by/4.0/>. The Creative Commons Public Domain Dedication waiver (<http://creativecommons.org/publicdomain/zero/1.0/>) applies to the data made available in this article, unless otherwise stated in a credit line to the data.

(Continued from previous page)

Conclusions: Autologous ADSCs can be used in combination with ShakeGel™3D to maintain functionality and create a viable three-dimensional growth environment. The combined transplantation of autologous ADSCs and ShakeGel™3D promotes the recovery of damaged endometrial tissue by increasing BMP7-Smad5 signal transduction, resulting in endometrium thickening, increased number of glands, and decreased fibrosis, leading to restoration of partial fertility.

Keywords: Autologous adipose-derived stem cells, ShakeGel™3D, Intrauterine adhesion, BMP7-Smad5 signaling pathway

Background

Intrauterine adhesions (IUA), the most common cause of uterine infertility, partially or completely block the uterine cavity and/or cervical canal and are caused by endometrial basal layer injury. There are several hypotheses about the pathogenesis of IUA, including the fibrosis hyperplasia theory, the neural reflex theory, abnormal differentiation of stem cells, changes in the uterine microenvironment and fibrosis, abnormal regulation of signaling pathways, and inflammatory response caused by adherent fibroblasts. Since the pathological features of IUA are endometrial fibrosis, the fibrosis hyperplasia theory is the most widely studied hypothesis. As a serious complication of uterine surgery, IUA can cause a plethora of female reproductive system health problems, such as menstrual abnormalities, recurrent abortion, periodic abdominal pain, infertility, and pregnancy-related complications. Therefore, the goal of IUA therapy is to reconstruct the normal uterine cavity and restore uterine function. The traditional treatment for this disease is hysteroscopic resection of transcervical adhesion, combined with various adjuvant therapies. However, some shortcomings and deficiencies of these anti-adhesion strategies, such as resistance to secondary surgery, limited isolation area, induction of intrauterine inflammatory response, and difficulty in endometrial regeneration, have forced researchers to continue to explore new treatment options.

Mesenchymal stem cells (MSCs) have the ability of multipotent differentiation, they can promote tissue repair, and they are characterized by low immunoreactivity and high immunosuppression. They are a suitable source of stem cells for the treatment of intrauterine adhesions. However, the safety of allogeneic MSCs regeneration therapy remains controversial. Compared with autologous MSCs, allogeneic MSCs have a higher risk of initiating an immune response [1], higher morbidity [2], and secondary cancers that may occur after allogeneic stem cell transplantation [3]. According to recent experiments and reports, autologous MSCs seem to be more suitable for the treatment of diseases [4–7]. Adipose-derived stem cells (ADSCs), a type of MSCs, have shown promise in regenerative medicine. In preclinical animal

models, autologous ADSCs are used to repair articular cartilage defects [8], enhance the recovery of erectile function after cavernous nerve injury [9], and repair Achilles tendon defects [10]. Furthermore, autologous ADSCs have been used in the treatment of Crohn's disease anal fistula [11], systemic sclerosis [12], and tracheomediastinal fistula in humans [13]. In addition, we reviewed the application of MSCs in female reproductive diseases [14]. Currently, the primary mechanisms of MSCs therapy have not been fully elucidated. The main mechanisms include differentiation into targeted cells, immunomodulatory interactions with multiple immune cells, homing and engraftment at targeted injury sites, and paracrine effects of various factors, among which the paracrine effect is the most likely mode of action.

In order to improve the local persistence and utilization rate of MSCs in the endometrium, scientists have used materials such as collagen scaffolds [15–17], hydrogel scaffolds [18], and platelet-rich plasma [19] to loaded with MSCs to restore the structure and function of the endometrium. Our experiments used a material with a three-dimensional polymeric network, a bioactive hydrogel mimicking the microenvironment and microstructure of tissues, supporting 3D tissue-like growth in vitro and in vivo [20]. ShakeGel™3D can also improve the proliferation or differentiation of stem cells.

Bone morphogenetic protein 7 (BMP7) is a member of the transforming growth factor (TGF) superfamily and a natural negative regulator of the TGF/Smad signaling pathway. Recently, a number of studies have found that BMP7 can inhibit the progression of cardiac fibrosis [21], glomerular and interstitial fibrosis in mouse models of chronic renal disease [22, 23], pulmonary fibrosis [24], and IUA [25]. Furthermore, experiments have shown that BMP7 may suppress TGF- β 1, which mediates IUA fibrosis by stimulating Smad and downstream regulatory pathways [26–30], inducing the process by regulating Smad5 to repair tissues [25].

In this study, we evaluated the therapeutic effects of a complex of mouse autologous ADSCs loaded on ShakeGel™3D in an IUA mouse model by activating the BMP7-Smad5 signaling pathway, which increased local perseverance and stem cells activity. We also aimed to

analyze whether transplantation of autologous ADSCs combined with ShakeGel™3D could improve the fertility of IUA mice.

Materials and methods

Experimental animals

All animal experimental protocols were approved by the Second Affiliated Hospital of Fujian Medical University Animal Care Committee and were in accordance with the National Institutes of Health Guide for the Care and Use of Laboratory Animals (number 97). Mice were kept in standard cages at 22 °C with a 12-h light-dark cycle and were allowed unlimited access to food and water.

Autologous ADSC preparation and identification

Mouse autologous ADSCs were prepared and cultured as described in previous studies [31–33]. Briefly, inguinal adipose tissue was obtained from female C57BL/6 mice 3–4 weeks of age, and each mouse was given an ear tag with a certain number on it. Fat tissue was collected and enzymatically digested with 0.75 mg/mL collagenase type II (Sigma) for 30 min at 37 °C. Immediately after digestion, the sample was centrifuged, and the precipitate was retained. For culture, the precipitate was rinsed twice in PBS, and the cell pellet was re-suspended in DMEM/F12 (1:1) (Hyclone) containing 10% fetal bovine serum (Gibco), 1% pen-strep (Gibco) and cultured at 37 °C in a 5% CO₂ humidified incubator. Flow cytometric analysis was used to identify cell surface markers of ADSCs, including CD105 (BioLegend), CD29 (BioLegend), CD75 (BioLegend), CD34 (BioLegend), and CD45 (BioLegend). Cells were treated with commercial osteogenic, chondrogenic, or adipogenic medium (Cyagen) for up to 24 days, following the manufacturer's instructions. The ability of ADSCs to differentiate through adipogenesis, osteogenesis, and chondrogenesis was visualized by Oil Red O staining, Alizarin red staining, and Alcian blue staining (Cyagen), respectively. Autologous ADSCs from passage 3 were used for experiments.

Preparation of the mouse autologous ADSCs combined with ShakeGel™3D complex

The complex was made as follows: First, the ShakeGel™3D (Biomaterials USA) solution, which has been reported to improve cell culture strategies [20], was gently mixed with the cell suspension into a centrifuge tube. Second, cell culture wells were pre-wet with 1× sterile PBS, and then the gel-cell mixture was rapidly added to the well and the mix was gently rocked back and forth to spread the mixture evenly across the surface of the well. Third, incubation followed at 37 °C for 5–10 min for hydrogel formation. Fourth, culture medium was added along the plate wall, followed by incubation at 37 °C in a humidified atmosphere containing 5% CO₂.

Finally, after 24 h, half the volume of the old medium was discarded, and the same amount of fresh medium was added. After that, the medium was refreshed every 24 h. According to the manufacturer's protocol, Calcein AM (Abcam) was used to examine cell viability, and cell counting Kit-8 (CCK-8) (Dojindo) was used to evaluate the proliferation of ADSCs. Three samples from each group were assessed using the CCK-8 assay ($n = 3$).

Establishment of IUA model

When the cells reached the second generation, which is approximately 6 or 7 weeks in a state of diestrus cycles of mice with consecutive 4-day estrus cycles [34], the IUA mouse model was established according to previous research [34]. Seven days after the surgery, the autologous ADSCs were cultured to the third generation. The mice ($n = 50$) were subdivided into 5 groups: sham operation group (sham group, $n = 10$), where mice had laparotomy without any treatment; PBS model group (PBS group, $n = 10$), where mice underwent induction of intrauterine adhesions, and, 7 days after modeling, a relaparotomy was performed and the mice were injected with 10 µl PBS in each of the two uterine horns; autologous ADSCs treatment group (ADSCs group, $n = 10$), where a relaparotomy was performed after 7 days of modeling, and autologous ADSCs (5×10^6 suspended in 10 µl PBS) [35] were injected into each of the two uterine horns, one by one, according to the mouse's ear tag; ShakeGel™3D model group (Gel group, $n = 10$), where mice underwent induction of intrauterine adhesions 7 days after modeling, a relaparotomy was performed, and the mice were injected with 10 µl ShakeGel™3D in each of the two uterine horns; and ADSCs combined with ShakeGel™3D treatment group (ADSCs + Gel group, $n = 10$), where a relaparotomy was performed after 7 days of modeling, and ADSCs combined with ShakeGel™3D (5×10^6 suspended in 10 µl ShakeGel™3D) were injected into each of the two uterine horns, one by one, according to the mouse's ear tag. Seven days after treatment, 25 mice ($n = 5$ per group) were sacrificed, their uterine tissues were harvested for the next experiment, and the other 25 remained for mating experiments. The study design is shown in Fig. 1.

GFP labeling of ADSCs

The green fluorescent protein (GFP) of a lentivirus (OBIO Technology) was stored at – 80 °C. According to the manufacturer's protocol, after 72 h of virus infection, the cells were observed under a fluorescence microscope to determine the efficiency of cell infection. These cells were then injected into the uterus.

Hematoxylin and eosin (H&E) staining

Uteri were fixed in 4% paraformaldehyde for 24 h and embedded in paraffin. The slides were first

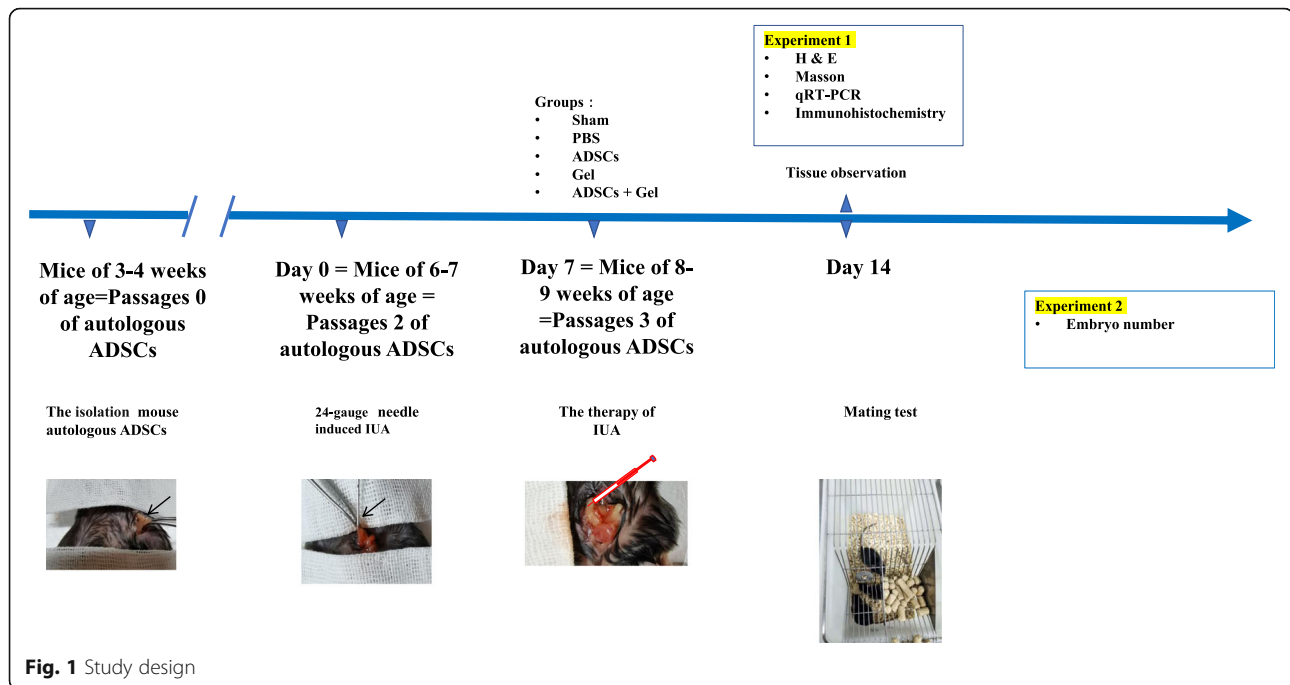


Fig. 1 Study design

deparaffinized and rehydrated, and then stained with H&E (Solarbio). We visualized the whole image of the pathological uterus and counted the gland quantity to predict IUA. Image-pro plus 6.0 was used to calculate the number of glands and endometrial thickness, and 3–5 fields were randomly selected from each slide to determine the mean number of glands and mean endometrial thickness.

Masson staining

Masson staining was used to detect endometrial fibrosis. The deparaffinized and rehydrated slides were incubated with Masson staining mixture (Solarbio) for 5 min and then stained with phosphomolybdic acid-aniline blue solution (Solarbio) for 5 min. The areas of the collagen fibers stained in blue relative to the total view were calculated.

Quantitative real-time polymerase chain reaction (qRT-PCR)

Total RNA was extracted from macrophages using the Mini BEST Universal RNA Extraction Kit (TaKaRa). RNA purity and concentration were measured using a spectrophotometer. Reverse transcription and cDNA synthesis were performed using PrimeScript™ RT reagent Kit with gDNA Eraser (Perfect Real Time) (Takara, Japan) according to the manufacturer’s instructions. The mRNA expression of α-SMA, TGF-β1, Smad-5, and BMP7 was quantified by qRT-PCR with TB Green® Premix Ex Taq™ (TliRNaseH Plus) (Takara), and the house-keeping gene, glyceraldehyde 3-phosphate

dehydrogenase (GAPDH), was used as an internal control for mRNA abundance. The sequences of the forward and reverse primers are shown in Table 1. Each group included six samples, and each sample was performed in triplicate. Relative gene expression between groups was calculated using the 2^{-ΔΔCT} method.

Immunohistochemistry

After deparaffinization, dehydration, and antigen retrieval, the slides were immersed in 3% hydrogen peroxide to block endogenous peroxidase activity, and then they were blocked in goat serum for 1 h. The slides were then incubated overnight at 4 °C with primary antibodies against α-smooth muscle actin (α-SMA, Abcam, 1:2000),

Table 1 qRT-PCR Forward/Reverse(F/R) primers sequences

Primers	Sequences 5'-3'
a-SMA	F: 5'- GCGTGGCTATTCCCTCGTACTAC -3'
	R: 5'- CGTCAGGCAGTTCGTAGCTCTTC -3'
TGF-β1	F: 5'- CCAGATCCTGTCCAAACTAAGG -3'
	R: 5'- CTCTTAGCATAGTAGTCCGCT -3'
BMP7	F: 5'- GATCCTGTCCATCTTAGGGTTG -3'
	R: 5'- GTTGACAGGTCCAACATGAAC -3'
Smad5	F: 5'- TTTCCCTTATCTCCTAACAGC -3'
	R: 5'- TACTGCTGTATCCATAGGCTG -3'
GAPDH	F: 5'- TGGGTGTGAACCATGAGAAG -3'
	R: 5'- GCTAAGCAGTTGGTGGTGC -3'

a-SMA a-smooth muscle actin, TGF-β1 transforming growth factor beta receptor 1, BMP7 bone morphogenetic protein 7, Smad5 SMAD family member 5, GAPDH glyceraldehyde-3-phosphate dehydrogenase

TGF- β 1 (Abcam,1:500), BMP7 (Abcam, 1 μ g/ml), and Smad5 (Abcam, 1:800). The sections were then incubated with appropriate secondary antibodies for 60 min at room temperature. The slides were then stained with 3, 3-diaminobenzidine (DAB) at room temperature, lightly counterstained with hematoxylin, dehydrated, and covered with glass cover slips. Quantification of immunoreactivity was performed using Image Pro-Plus 6.0, and 3–5 fields were randomly selected from each slide to determine the mean optical density (MOD).

Statistical analysis

Data were analyzed using the *F* test with subsequent *t*-tests (equal variance) for the comparison between two different groups. For three or more groups, an ANOVA test was used, followed by the least significant differences method. GraphPadPrism8 (GraphPad Software Inc., La Jolla, CA, USA) was used to obtain graphs and statistics. Significant values were designated as follows: **p* < 0.05, ***p* < 0.01, ****p* < 0.001, and *****p* < 0.0001. All data are shown as the mean \pm standard deviation (SD).

Results

Characterization and differentiation of autologous ADSCs and their safety assessment on ShakeGel™3D

The appearance of autologous ADSCs from passage 0 (P0) to P3, especially the third passage, gradually came to resemble typical spindle-shaped fibroblast-like cells that were arranged closely with vortex-like growth (Supplementary figure S1.1). In the third passage, fluorescence-activated cell sorting (FACS) showed that autologous ADSCs expressed CD105 (99.1%), CD29 (99.6%), CD73 (98.9%), CD34 (0.46%), and CD45 (3.26%) (Supplementary figure S1.2). In addition, these cells were

successfully induced to become adipocytes, osteoblasts, and chondroblasts in vitro (Supplementary figure S1.3).

To further evaluate the safety of autologous ADSCs on ShakeGel™3D, the live-dead cell staining results (Fig. 2) showed that these cells showed aggregation of globulin in the ShakeGel™3D, and a small number of fibrous fat stem cells were extended at the junction between the ShakeGel™3D edge and the cell culture base. On day seven in the ShakeGel™3D culture environment, autologous ADSCs showed good activity and could continue to proliferation in the shaker environment. In addition, the CCK-8 results (Fig. 3) verified that the OD value of cells cultured by 5×10^6 cells + ShakeGel™3D was higher than that by 1×10^6 cells + ShakeGel™3D. On the third day of co-culture, the OD value began to increase gradually. By the seventh day, the OD value of 5×10^6 cells + ShakeGel™3D was over 50%.

The IUA models the effect of autologous ADSCs on ShakeGel™3D

First, to locate the autologous ADSCs/GFP in the uterus, as expected, we did not observe any GFP-positive cells in the uterine tissue sections of the sham, PBS, and Gel groups. However, we observed GFP-positive cells in the uterine tissue sections of the ADSCs group (2.175%) and ADSCs + Gel group (9.215%). Furthermore, GFP-positive cells in the uterine tissue sections of the ADSCs + Gel group were higher than that in the ADSCs group (*P* = 0.0101) (Fig. 4).

The macroscopic appearance of the uterus sham groups was smoother than in the PBS group. On day 7 from ADSCs transplantations, ShakeGel™3D, or ADSCs combined with ShakeGel™3D, the macroscopic appearance of the uterus gradually recovered, similar to that of a normal uterus (Fig. 5.1). H&E staining of the uterine

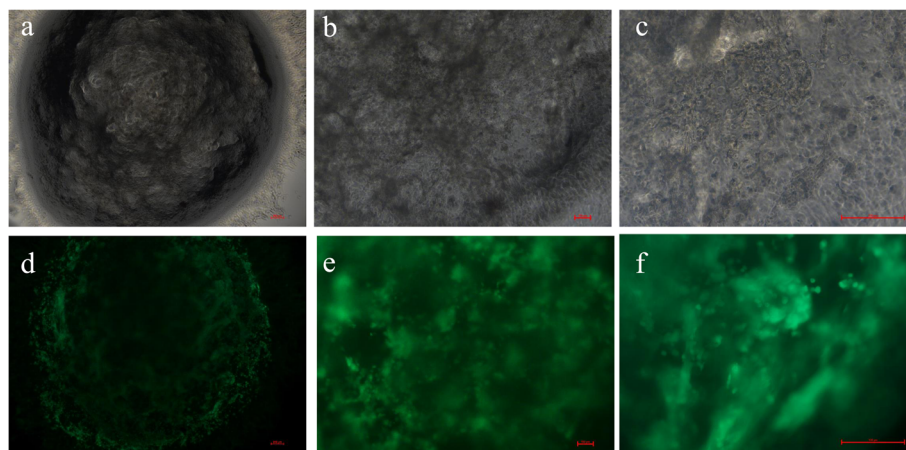
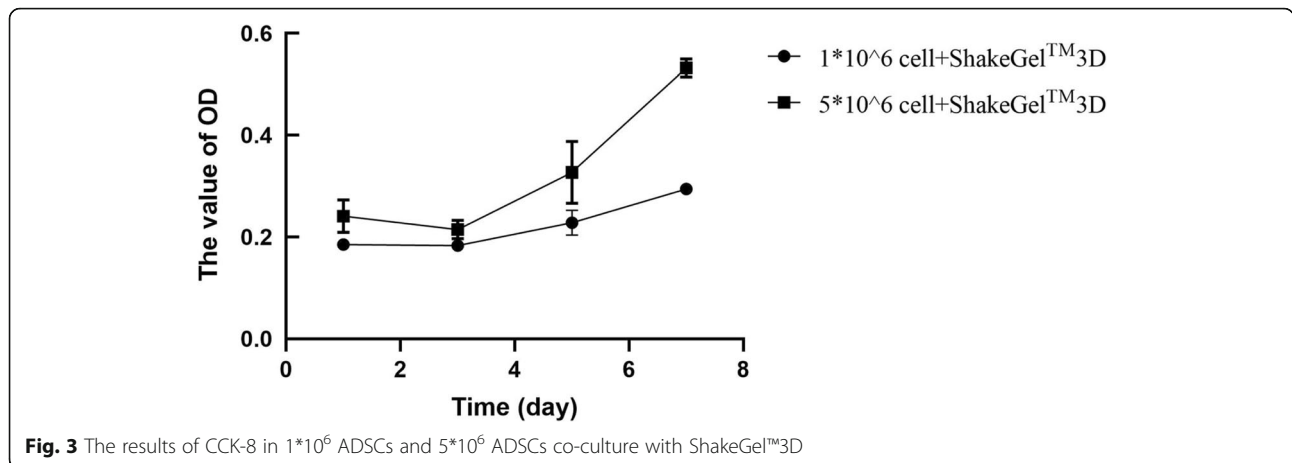


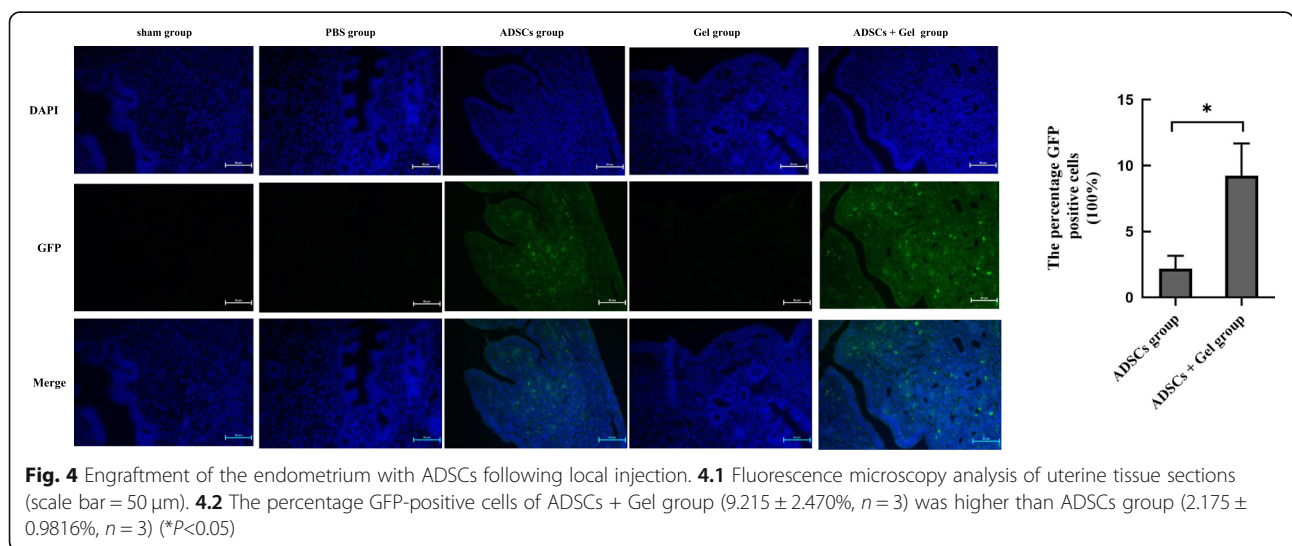
Fig. 2 Assay of the activity of ADSCs combined with ShakeGel™3D. **a**, **b**, and **c** respectively were ADSCs combined with ShakeGel™3D under white light 4 \times , 10 \times , and 20 \times . **d**, **e**, and **f** respectively were ADSCs combined with ShakeGel™3D under active staining 4 \times , 10 \times , and 20 \times (scale bar = 100 μ m)

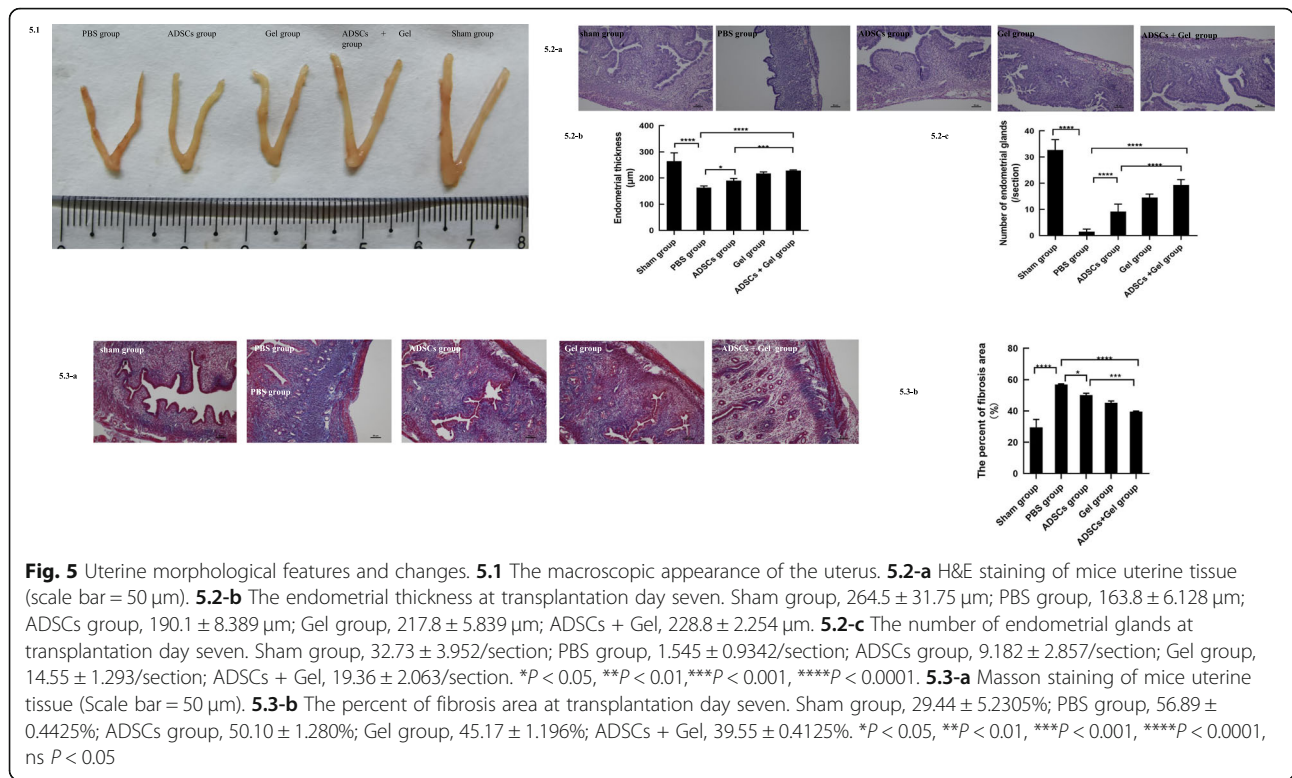


tissue showed that the endometrial thickness (163.8 ± 6.128 μm) of the PBS group showed significant differences when compared with the thickness (264.5 ± 31.75 μm) of the sham group (*P* < 0.0001) (Fig. 5.2). When transplanted with ADSCs or ADSCs combined with ShakeGel™3D, thickness increased significantly compared to the PBS group (ADSCs group 190.1 ± 8.389 μm, *P* < 0.05; ADSCs + Gel group 228.8 ± 2.254 μm, *P* < 0.0001). The endometrium regenerated in the ADSCs + Gel group was thicker than that in the ADSCs group (*P* < 0.001) (Fig. 5.2). Further, when comparing to endometrial tissues of the PBS group, gland numbers were increased in the ADSCs group (9.182 ± 2.857 versus 1.545 ± 0.9342, respectively, per unit area, *P* < 0.0001), Gel group (14.55 ± 1.293 versus 1.545 ± 0.9342, respectively, per unit area, *P* < 0.0001), and ADSCs + Gel group (19.36 ± 2.063 versus 1.545 ± 0.9342, respectively, per unit area, *P* < 0.0001). Compared with the ADSCs group, the gland numbers of ADSCs +Gel

were increased (*P* < 0.0001). To further evaluate the degree of fibrosis, Masson’s trichrome staining was performed. As shown in Fig. 5.3, a large amount of fibrous tissue appeared in the PBS group (56.89 ± 0.4425%), compared to the sham group (29.44 ± 5.2305%). Interestingly, the percentage of fibrosis area was decreased after ADSCs (50.10 ± 1.280%, *P* < 0.05), ShakeGel™3D (45.17 ± 1.196%, *P* < 0.0001) or ADSCs combined with ShakeGel™3D (39.55 ± 0.4125%, *P* < 0.0001) treatment compared with the PBS group. In addition, the percentage of fibrosis area in the ADSCs +Gel group was significantly less than that of the ADSCs group (*P* < 0.001).

To further confirm the results of the fibrosis of experiments, we detected α-SMA expression and mean optical density of α-SMA in endometrium (Fig. 6). All these valuations indicated that the fibrosis in the ADSCs + Gel group was significantly smaller than in the ADSCs group. In addition, expression of TGF-β1, an archetypical promoter of fibrosis, (Fig. 6.2-b) was significantly





less in the ADSCs + Gel group than in the ADSCs group, as shown by qRT-PCR (Fig. 7.1-b) and IHC experiments. The mating experiments showed that only the Sham group and ADSCs + Gel group achieved pregnancy (Fig. 7.2).

ADSCs combined with ShakeGel™3D treatment enhance BMP7-Smad5 signaling

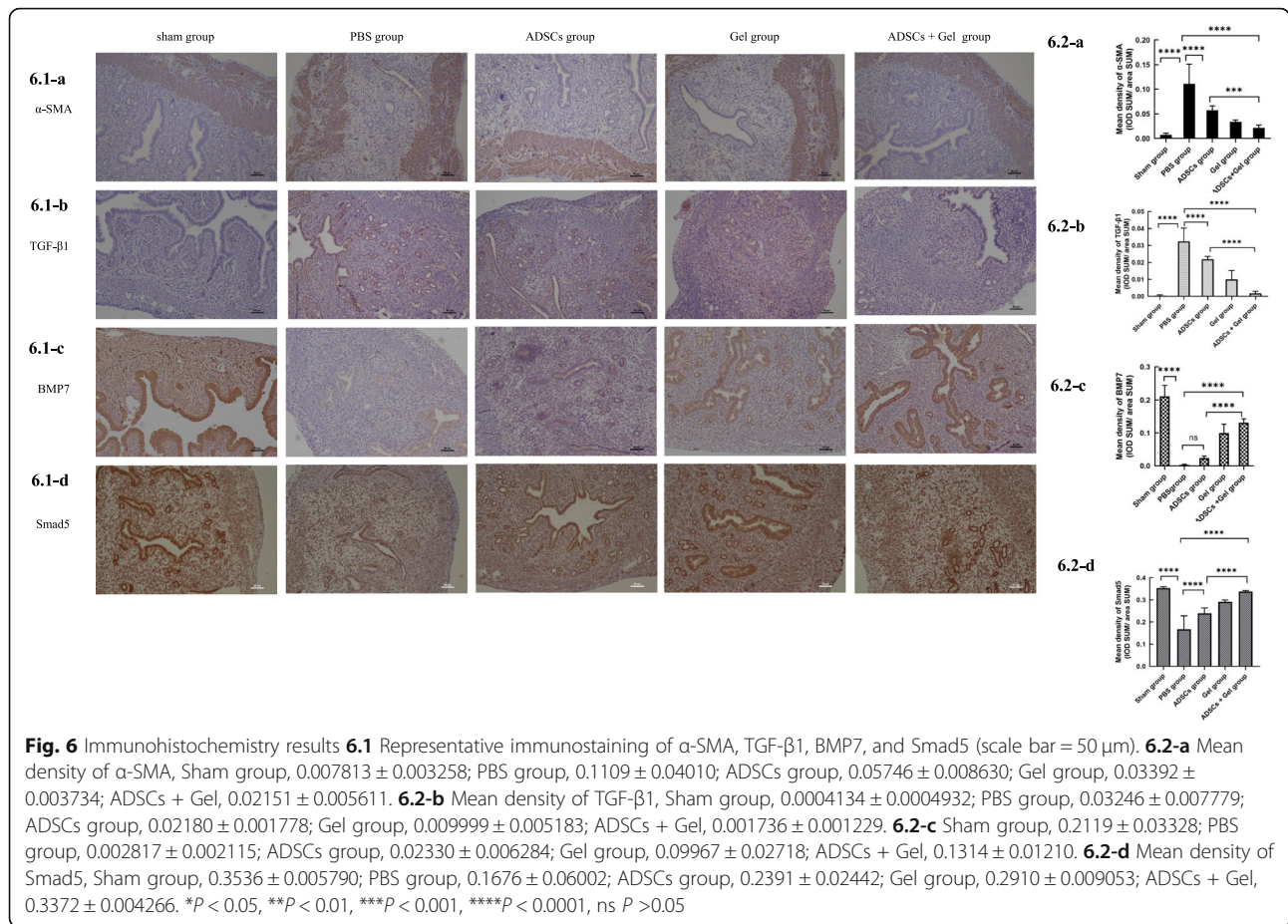
The qRT-PCR results (Fig. 7.1) showed that BMP7 expression in the ADSCs group (0.06124 \pm 0.006388) was slightly higher than in the PBS group (0.05062 \pm 0.01281), but the difference was not statistically significant (P = 0.5302). BMP7 expression was higher in ADSCs + Gel group (0.5575 \pm 0.06289) than in the PBS group. The difference was statistically significant (P < 0.0001). The ADSCs + Gel group was also statistically significant compared to the ADSCs group (P < 0.0001). Similarly, Smad5 expression in the ADSCs group (0.7127 \pm 0.05734) was slightly higher than in the PBS group (0.6843 \pm 0.07691), but the difference was not statistically significant (P = 0.9820). The mRNA expression of Smad5 in the ADSCs + Gel group (0.9066 \pm 0.07593) was significantly higher than in the PBS group (P < 0.01). The ADSCs + Gel group result was also statistically significant compared with ADSCs (P = 0.0167).

Likewise, for immunohistochemistry results, the staining intensity for BMP7 in the ADSCs group (0.02330 \pm 0.006284) was slightly higher than that in the PBS group

(0.002817 \pm 0.002115), but the difference was not statistically significant (P = 0.1739). BMP7 expression was higher in the ADSCs + Gel group (0.1314 \pm 0.01210) than in the PBS group. The difference was statistically significant (P < 0.0001). Compared with the ADSCs group, the ADSCs + Gel group expression was significantly higher (P < 0.0001). The mean density of Smad5 in the PBS group (0.1676 \pm 0.06002) was lower than in the ADSCs group (0.2391 \pm 0.02442, P < 0.0001), Gel group (0.2910 \pm 0.009053, P < 0.0001), and ADSCs + Gel group (0.3372 \pm 0.004266, P < 0.0001). The mean density of Smad5 in the ADSCs + Gel group was significantly higher than in the ADSCs group (P < 0.0001) and Gel group (P = 0.0087).

Discussion

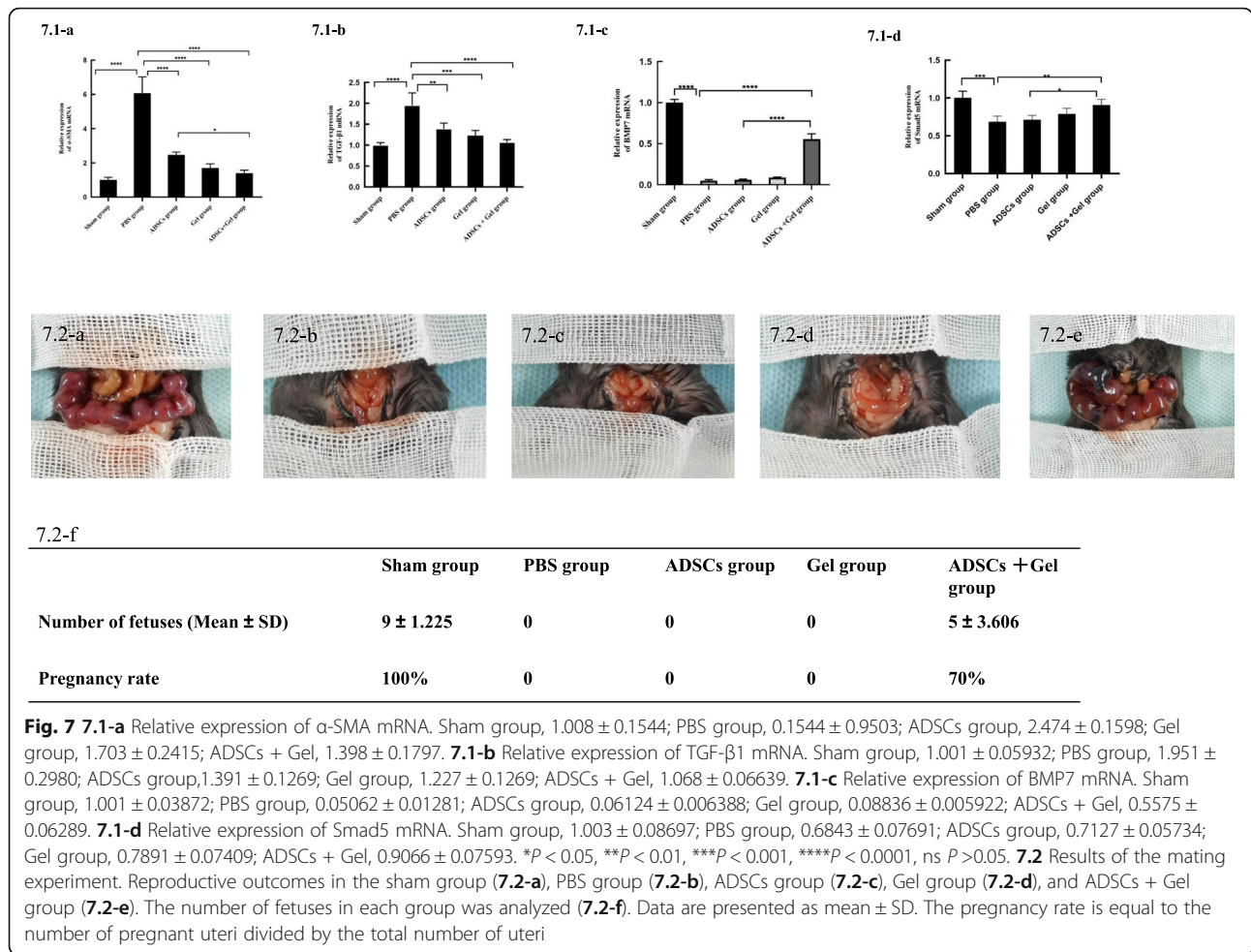
In this study, we have demonstrated that (1) the combination of ShakeGel™3D and autologous ADSCs can achieve good results, thereby creating a feasible three-dimensional growth environment; (2) autologous ADSCs combined with ShakeGel™3D can promote the recovery of injured endometrial tissue, thus increasing the thickness of the endometrium, increasing the number of glands and reducing fibrosis; and (3) compared with other treatment groups, the combination of autologous ADSCs and ShakeGel™3D grafts can increase the expression of BMP7 and Smad5, indicating that the combination of autologous ADSCs and ShakeGel™3D grafts can



promote endometrial repair through the BMP7-Smad5 signaling pathway.

Stem cells, including MSCs, are one of the most promising tools, and they have been applied to various tissues for regenerative medicine and cell therapy, including the uterus endometrium regeneration [35, 36]. ADSCs can be isolated from white adipose tissue in large quantities, and autologous transplantation can be realized. Some studies have shown that the application of allogeneic stem cell therapy has some risks, including abnormal immune reconstitution, secondary cancer, and graft-versus-host disease [3, 37, 38]. Our study is the first to use autologous ADSCs to treat intrauterine adhesions in mice. In our study, we used autologous ADSCs combined with ShakeGel™3D, which has proven that it can support the microenvironment and tissue microstructure for cells to improve proliferation [20]. The CCK-8 results of our study showed that autologous ADSCs still proliferate in ShakeGel™3D. Furthermore, the effects of the group with autologous ADSCs combined with ShakeGel™3D were confirmed by histological inspection and detection of some fiber correlation factors. In addition, compared with the ADSCs and the Gel groups, the ADSCs + Gel group had more GFP-positive cells in the

endometrial tissue, thickened endometrium, increased endometrial glands, decreased fibrotic area, and α-SMA and TGF-β1 expression. These results suggest that the ShakeGel™3D not only acts as a physical barrier to IUA, but also provides an ideal attachment site for ADSCs to maintain a high density in the uterine cavity, thereby improving reconstruction of abnormal tissue. Further, GFP positive cells were observed in the stromal compartment, consistent with a previous report [39]. We suggested that ADSCs may provide paracrine support for the epithelial cells to regenerate. Transplanted ADSCs may release bioactive molecules, including growth factors, cytokines, chemokines, and stem cell mobilizing factors that are beneficial to the IUA by paracrine mechanisms. Although Liu et al. concluded that systemic administration can recruit MSCs to the injured uterus better than local injection [35], vein engraftment of stem cells in the damaged area cannot be guaranteed. In fact, the majority of the stem cells after intravenous injection are trapped in the lungs, and the number of MSCs that home to the endometrium is very small [35, 39]. In addition, in our research, ShakeGel™3D serves as a slow-release stem cell scaffold, allowing ADSCs to continuously secrete factors to promote endometrial repair. Therefore, we used local



injection of autologous ADSCs combined with ShakeGel™3D to treat IUA.

Interestingly, our study also showed that the Gel group without any therapeutic cells showed better performance (thicker endometrium, more glands, less fibrosis area after treatment) than the ADSCs group. We suggested that ShakeGel™3D acted as a physical barrier to IUA, retarded adverse remodeling processes, and provided an ideal extracellular environment for the remaining endometrial stromal cells. To figure out why ShakeGel™3D solely helps the endometrium regeneration, more researches need to be done. In addition, all kinds of hydrogel, as a stand-alone therapy, have been used in IUA human [40], which cannot completely eliminate IUA, but can attenuate the deterioration of adhesions. Further, many researchers have combined hydrogel biomaterials with stem cells, growth factors, and other components to treat diseases.

Abnormal repair and fibrosis after endometrial surgery can lead to intrauterine adhesion damage, which is pathologically similar to all fibrotic lesions, including the extracellular matrix, excessive accumulation of tissue

remodeling, and scar formation [41]. Therefore, for IUA therapy, blocking the formation of fibrosis plays a key role. TGF- β 1 has been shown to promote endometrial fibrosis in IUA patients and animal models [42]. Some researchers have proved that TGF- β 1 influences tissue fibrosis via Smad2, Smad3, Smad7 signaling [43]. However, a previous study showed that the expression of BMP7, another member of the TGF- β superfamily, was negatively correlated with Smad5 in IUA. BMP7-Smad5 signal transduction occurs in endometrial fibrosis and has an anti-fibrotic effect in IUA [25]. Our study used mechanical trauma to establish a mouse model of IUA. We found that, compared with the PBS group, both the mRNA and protein BMP7 levels in the ADSCs + Gel group increased. At the same time, the level of Smad5 consistent with that of BMP7 also increased. Compared with the PBS group, the levels of BMP7 and Smad5 in the ADSCs group increased slightly, but the difference was no statistically significant. Our study shows for the first time that the combination of ADSCs and ShakeGel™3D can treat IUA by changing the BMP7-Smad5 signaling pathway. Furthermore, we suggest that the gel can improve the function of ADSCs.

We outline next few steps in our ongoing research to further elucidate the mechanism of ADSCs combined with gel in the treatment of intrauterine adhesions. First, due to the extreme challenge of preparing an appropriate number of autologous ADSCs, we plan to isolate and purify exosomes from ADSCs in place of cell therapy for IUA. In addition, we may be able to identify key factors in the release of ADSCs during endometrial recovery. Second, we have just completed a mouse study, and we are planning to treat IUA with autologous ADSCs combined with ShakeGel™3D in a large animal model more similar to the pathophysiology of the endometrium of human females. In addition, randomized controlled trials are needed to confirm the therapeutic role of ADSCs in fertility medicine.

Conclusion

In this study, it was shown that both autologous ADSCs and autologous ADSCs combined with ShakeGel™3D could repair IUA caused by mechanical injury. Since ShakeGel™3D enhances the function of ADSCs, autologous ADSC transplantation combined with ShakeGel™3D holds significant advantages in anti-fibrotic repair and promotion of endometrial regeneration by altering the BMP7-Smad5 signaling pathway. These data are helpful in treating intrauterine adhesions.

Abbreviations

IUA: Intrauterine adhesions; MSCs: Mesenchymal stem cells; ADSCs: Adipose-derived stem cells; BMP7: Bone morphogenetic protein 7; TGF: Transforming growth factor

Supplementary Information

The online version contains supplementary material available at <https://doi.org/10.1186/s13287-021-02258-0>.

Additional file 1: Supplementary figure S1. S1.1 The appearance of autologous ADSCs of passage 0 (P0) to P3. The cells at third passage showed homogenous fibroblastic morphology. **S1.2** Adipose tissue derived mesenchymal stem cell identification with flow cytometry. CD105: 99.1%, CD29: 99.6%, CD73: 98.9%, CD34: 0.46%, CD45: 3.26%. **S.3** The differentiation of ADSCs. Under the white light, The differentiated adipocytes secreted lipid droplets (a-1, a-2). Oil Red-O staining adipogenic differentiation (b-1, b-2). Alizarin red staining indicated osteogenic differentiation (c-1, c-2). Alcian blue staining indicated chondrogenic differentiation (d-1, d-2).

Acknowledgements

Not applicable.

Authors' contributions

Shu Lin, Qi-yang Shi, Hong-zhi Gao, and Shao-rong Chen designed the study methodology. Yun-xia Zhao, Qiao-yi Huang, Wei-can Chen, Tian Xia, and Yan-chuan Shi collected the data and analyzed the results. Yun-xia Zhao drafted the article. All authors reviewed and revised the work. All authors reviewed the final article and approved it for submission.

Funding

This work was supported by 2020CT003, BS202007, 2018N019S, and 2018-CX-34.

Availability of data and materials

The data that support the findings of this study are available from the corresponding author upon reasonable request.

Declarations

Ethics approval and consent to participate

All animal procedures reported in this study have been approved by the Second Affiliated Hospital of Fujian Medical University Animal Care Committee under protocol number 97.

Consent for publication

Not applicable

Competing interests

There is no conflict of interest to declare.

Author details

¹Department of Gynaecology and Obstetrics, The Second Affiliated Hospital of Fujian Medical University, No.34 North Zhongshan Road, Quanzhou 362000, Fujian Province, China. ²Department of Anaesthesiology, the Second Affiliated Hospital, Fujian Medical University, Quanzhou, China. ³School of Pharmaceutical Sciences, Xiamen University, Xiamen 361102, Fujian province, China. ⁴Diabetes and Metabolism Division, Garvan Institute of Medical Research, 384 Victoria Street, Darlinghurst, Sydney, NSW 2010, Australia. ⁵Faculty of Medicine, St Vincent's Clinical School, University of New South Wales, Sydney, New South Wales 2052, Australia. ⁶Clinical Center for Molecular Diagnosis and Therapy, the Second Affiliated Hospital of Fujian Medical University, Quanzhou, Fujian, China. ⁷Centre of Neurological and Metabolic Research, the Second Affiliated Hospital of Fujian Medical University, No.34 North Zhongshan Road, Quanzhou 362000, Fujian Province, China.

Received: 8 January 2021 Accepted: 1 March 2021

Published online: 18 March 2021

References

- Rowe JM, Ciobanu N, Ascensao J, Stadtmayer EA, Weiner RS, Schenkein DP, et al. Recommended Guidelines for the Management of Autologous and Allogeneic Bone Marrow Transplantation A Report from the Eastern Cooperative Oncology Group (ECOG); 2018. p. 143–58.
- Majhail NS, Mau LW, Denzen EM, Arneson TJ. Costs of autologous and allogeneic hematopoietic cell transplantation in the United States: a study using a large National Private Claims Database; 2013. p. 294–300.
- Mohty B, Mohty M. Long-term complications and side effects after allogeneic hematopoietic stem cell transplantation: an update. *Blood Cancer J.* 2011;1 [cited 2020 Nov 30]. Available from: <http://www.ncbi.nlm.nih.gov/pubmed/22829137>.
- Lu M, Peng L, Ming X, Wang X, Cui A, Li Y, et al. Enhanced wound healing promotion by immune response-free monkey autologous iPSCs and exosomes vs. their allogeneic counterparts. *EBioMedicine.* 2019;42:443–57 Elsevier B.V. Available from: <https://doi.org/10.1016/j.ebiom.2019.03.011>.
- Riccobono D, Agay D, Scherthan H, Forcheron F, Vivier M, Ballester B, et al. Application of adipocyte-derived stem cells in treatment of cutaneous radiation syndrome. *Health Phys.* 2012;103:120–6.
- Osborn TM, Hallett PJ, Schumacher JM, Isacson O. Advantages and recent developments of autologous cell therapy for Parkinson's disease patients. *Front Cell Neurosci.* 2020;14:1–13.
- Chang YW, Wu YC, Huang SH, Wang HMD, Kuo YR, Lee SS. Autologous and not allogeneic adipose-derived stem cells improve acute burn wound healing. *PLoS One.* 2018;13:1–16.
- Li Q, Zhao F, Li Z, Duan X, Cheng J, Zhang J, et al. Autologous fractionated adipose tissue as a natural biomaterial and novel one-step stem cell therapy for repairing articular cartilage defects. *Front Cell Dev Biol.* 2020;8:1–15.
- Qiu X, Fandel TM, Ferretti L, Albersen M, H O, Zhang H, et al. Both immediate and delayed intracavernous injection of autologous adipose-derived stromal vascular fraction enhances recovery of erectile function in a rat model of cavernous nerve injury. *Eur Urol.* 2012;62 [cited 2020 Nov 30]. Available from: <http://www.ncbi.nlm.nih.gov/pubmed/22397847>.
- Deng D, Wang W, Wang B, Zhang P, Zhou G, Zhang WJ, et al. Repair of Achilles tendon defect with autologous ASCs engineered tendon in a rabbit

- model. *Biomaterials*. 2014;35:8801–9 [cited 2020 Nov 30]. Available from: <http://www.ncbi.nlm.nih.gov/pubmed/25069604>.
11. Dige A, Hougaard HT, Agnholt J, Pedersen BG, Tencerova M, Kassem M, et al. Efficacy of injection of freshly collected autologous adipose tissue into perianal fistulas in patients with Crohn's disease. *Gastroenterology*. 2019;156:2208–2216.e1 [cited 2020 Nov 30]. Available from: <http://www.ncbi.nlm.nih.gov/pubmed/30772343>.
 12. Granel B, Daumas A, Jouve E, Harlé J-R, Nguyen P-S, Chabannon C, et al. Safety, tolerability and potential efficacy of injection of autologous adipose-derived stromal vascular fraction in the fingers of patients with systemic sclerosis: an open-label phase I trial. *Ann Rheum Dis*. 2015;74:2175–82 [cited 2020 Nov 30]. Available from: <http://www.ncbi.nlm.nih.gov/pubmed/25114060>.
 13. Álvarez PD, García-Araráz M, Georgiev-Hristov T, García-Olmo D. A new bronchoscopic treatment of tracheoemphysemic fistula using autologous adipose-derived stem cells. *Thorax*. 2008;63 [cited 2020 Nov 30]. Available from: <http://www.ncbi.nlm.nih.gov/pubmed/18364447>.
 14. Zhao Y-X, Chen S-R, Su P-P, Huang F-H, Shi Y-C, Shi Q-Y, et al. Using mesenchymal stem cells to treat female infertility: an update on female reproductive diseases. *Stem Cells Int*. 2019, 2019:9071720 [cited 2020 Dec 3]. Available from: <http://www.ncbi.nlm.nih.gov/pubmed/31885630>.
 15. Zhao G, Cao Y, Zhu X, Tang X, Ding L, Sun H, et al. Transplantation of collagen scaffold with autologous bone marrow mononuclear cells promotes functional endometrium reconstruction via downregulating Δ Np63 expression in Asherman's syndrome. *Sci China Life Sci*. 2017;60:404–16.
 16. Xin L, Lin X, Pan Y, Zheng X, Shi L, Zhang Y, et al. A collagen scaffold loaded with human umbilical cord-derived mesenchymal stem cells facilitates endometrial regeneration and restores fertility. *Acta Biomater*. 2019;92:160–71 *Acta Materialia Inc*. Available from: <https://doi.org/10.1016/j.actbio.2019.05.012>.
 17. Cao Y, Sun H, Zhu H, Zhu X, Tang X, Yan G, et al. Allogeneic cell therapy using umbilical cord MSCs on collagen scaffolds for patients with recurrent uterine adhesion: a phase I clinical trial. *Stem Cell Res Ther*. 2018;9:1–10.
 18. Huang Q, Zou Y, Arno MC, Chen S, Wang T, Gao J, et al. Hydrogel scaffolds for differentiation of adipose-derived stem cells. *Chem Soc Rev*. 2017;46:6255–75 *Royal Society of Chemistry*. Available from: <https://doi.org/10.1039/C6CS00052E>.
 19. Zhang S, Li P, Yuan Z, Tan J. Platelet-rich plasma improves therapeutic effects of menstrual blood-derived stromal cells in rat model of intrauterine adhesion. *Stem Cell Res Ther*. 2019;10:1–12.
 20. Chen H, Wei X, Chen H, Wei H, Wang Y, Nan W, et al. The study of establishment of an in vivo tumor model by three-dimensional cells culture systems methods and evaluation of antitumor effect of biotin-conjugated pullulan acetate nanoparticles. *Artif Cells Nanomedicine Biotechnol*. 2019;47:123–31 *Taylor & Francis*. Available from: <https://doi.org/10.1080/21691401.2018.1544142>.
 21. Towbin JA. Scarring in the heart — a reversible phenomenon? *N Engl J Med*. 2007;357:1767–8.
 22. Zeisberg M, Hanai JI, Sugimoto H, Mammoto T, Charytan D, Strutz F, et al. BMP-7 counteracts TGF- β 1-induced epithelial-to-mesenchymal transition and reverses chronic renal injury. *Nat Med*. 2003;9:964–8.
 23. Lin J, Patel SR, Cheng X, Cho EA, Levitan I, Ullenbruch M, et al. Kielin/chordin-like protein, a novel enhancer of BMP signaling, attenuates renal fibrotic disease. *Nat Med*. 2005;11:387–93.
 24. Myllärniemi M, Lindholm P, Rynnänen MJ, Klimont CR, Salmenkivi K, Keski-Oja J, et al. Gremlin-mediated decrease in bone morphogenetic protein signaling promotes pulmonary fibrosis. *Am J Respir Crit Care Med*. 2008;177:321–9.
 25. Guo LP, Chen LM, Chen F, Jiang NH, Sui L. Smad signaling coincides with epithelial-mesenchymal transition in a rat model of intrauterine adhesion. *Am J Transl Res*. 2019;11:4726–37.
 26. Yao Y, Chen R, Wang G, Zhang Y, Liu F. Exosomes derived from mesenchymal stem cells reverse EMT via TGF- β 1/Smad pathway and promote repair of damaged endometrium. *Stem Cell Res Ther*. 2019;10:1–17.
 27. Salma U, Xue M, Ali Sheikh MS, Guan X, Xu B, Zhang A, Huang L, Xu D. Role of Transforming Growth Factor- β 1 and Smads Signaling Pathway in Intrauterine Adhesion. *Mediators Inflamm*. 2016;2016:4158287. <https://doi.org/10.1155/2016/4158287>. Epub 2016 Feb 21. PMID: 26997760; PMCID: PMC4779532.
 28. Zhang Z, Li S, Deng J, Yang S, Xiang Z, Guo H, et al. Aspirin inhibits endometrial fibrosis by suppressing the TGF- β 1–Smad2/Smad3 pathway in intrauterine adhesions. *Int J Mol Med*. 2020;45:1351–60.
 29. Liu S, Huang X, Liu Y, Song D, Xiao Y. Functional analysis of miRNAs combined with TGF- β 1/Smad3 inhibitor in an intrauterine rat adhesion cell model. *Mol Cell Biochem*. 2020;470:15–28 *Springer US*. Available from: <https://doi.org/10.1007/s11010-020-03741-7>.
 30. Liu L, Chen G, Chen T, Shi W, Hu H, Song K, et al. si-SNHG5-FOXF2 inhibits TGF- β 1-induced fibrosis in human primary endometrial stromal cells by the Wnt/ β -catenin signalling pathway. *Stem Cell Res Ther*. 2020;11:1–17.
 31. Zuk PA, Zhu MI, Mizuno H, Huang J, Futrell JW, Katz AJ, et al. Multilineage cells from human adipose tissue: implications for cell-based therapies. *Tissue Eng*. 2001;7 [cited 2020 Dec 5]. Available from: <http://www.ncbi.nlm.nih.gov/pubmed/11304456>.
 32. Bunnell BA, Flaatt M, Gagliardi C, Patel B, Ripoll C. Adipose-derived stem cells: isolation, expansion and differentiation. *Methods*. 2008;45:115–20.
 33. Si Z, Wang X, Sun C, Kang Y, Xu J, Wang X, et al. Adipose-derived stem cells: sources, potency, and implications for regenerative therapies. *Biomed Pharmacother*. 2019;114:108765 *Elsevier*. Available from: <https://doi.org/10.1016/j.biopha.2019.108765>.
 34. Li B, Zhang Q, Sun J, Lai D. Human amniotic epithelial cells improve fertility in an intrauterine adhesion mouse model. *Stem Cell Res Ther*. 2019;10:1–14.
 35. Liu Y, Tal R, Pluchino N, Mamillapalli R, Taylor HS. Systemic administration of bone marrow-derived cells leads to better uterine engraftment than use of uterine-derived cells or local injection. *J Cell Mol Med*. 2018;22 [cited 2020 Dec 7]. Available from: <http://www.ncbi.nlm.nih.gov/pubmed/28782281>.
 36. Azizi R, Aghebaty-Maleki L, Nouri M, Marofi F, Negargar S, Yousefi M. Stem cell therapy in Asherman syndrome and thin endometrium: Stem cell-based therapy. *Biomed Pharmacother*. 2018;102 [cited 2020 Dec 26]. Available from: <http://www.ncbi.nlm.nih.gov/pubmed/29571018>.
 37. Campo H, Cervelló I, Simón C. Bioengineering the uterus: an overview of recent advances and future perspectives in reproductive medicine. *Ann Biomed Eng*. 2017;45 [cited 2020 Dec 26]. Available from: <http://www.ncbi.nlm.nih.gov/pubmed/28028711>.
 38. Bellm LA, Epstein JB, Rose-Ped A, Martin P, Fuchs HJ. Patient reports of complications of bone marrow transplantation. *Support Care Cancer*. 2000;8:33–9.
 39. Singh P, Bhartiya D. Pluripotent stem (VSELs) and progenitor (EnSCs) cells exist in adult mouse uterus and show cyclic changes across estrus cycle. *Reprod Sci*. 2021;28:278–90.
 40. Ludwin A, Ludwin I, Pityński K, Banas T, Jach R. Role of morphologic characteristics of the uterine septum in the prediction and prevention of abnormal healing outcomes after hysteroscopic metroplasty. *Hum Reprod*. 2014;29:1420–31.
 41. Wynn TA, Ramalingam TR. Mechanisms of fibrosis: therapeutic translation for fibrotic disease. *Nat Med [Internet]*. *Nat Publ Group*. 2012;18:1028–40 Available from: <https://doi.org/10.1038/nm.2807>.
 42. Salma U, Xue M, Ali Sheikh MS, Guan X, Xu B, Zhang A, et al. Role of transforming growth factor- β 1 and smads signaling pathway in intrauterine adhesion. *Mediat Inflamm*. 2016;2016 [cited 2020 Dec 26]. Available from: <http://www.ncbi.nlm.nih.gov/pubmed/26997760>.
 43. Abudukeyoumu A, Li MQ, Xie F. Transforming growth factor- β 1 in intrauterine adhesion. *Am J Reprod Immunol*. 2020;84:1–11.

Publisher's Note

Springer Nature remains neutral with regard to jurisdictional claims in published maps and institutional affiliations.

Ready to submit your research? Choose BMC and benefit from:

- fast, convenient online submission
- thorough peer review by experienced researchers in your field
- rapid publication on acceptance
- support for research data, including large and complex data types
- gold Open Access which fosters wider collaboration and increased citations
- maximum visibility for your research: over 100M website views per year

At BMC, research is always in progress.

Learn more [biomedcentral.com/submissions](https://www.biomedcentral.com/submissions)

